Dalton Transactions

ROYAL SOCIETY OF CHEMISTRY

PAPER

View Article Online
View Journal | View Issue

Cite this: *Dalton Trans.*, 2022, **51**, 4502

Application of NMR relaxometry for real-time monitoring of the removal of metal ions from water by synthetic clays†

Stefano Marchesi, ‡[a] Simone Nascimbene,‡[a] Matteo Guidotti, [b] Chiara Bisio *[a,b] and Fabio Carniato *[a]

Received 27th December 2021,
Accepted 13th February 2022

DOI: 10.1039/d1dt04344g

rsc.li/dalton

The removal of paramagnetic metal ions with different charges and ionic radii (*i.e.* Gd^{3+}, Cu^{2+}, and Co^{2+}) from aqueous solutions was carried out by using a Na^{+}-exchanged synthetic saponite clay. Saponite, composed of sub-micrometer particles and characterized by high cation-exchange capacity, was prepared through a classical low-cost hydrothermal approach. The metal ion uptake tests were performed in water at pH = 5.5 and 3.0, and the capture process was monitored in real time by ^{1}H-NMR relaxometry. The experimental data were confirmed by the conventional ICP-OES technique. Details of the uptake process kinetics were extrapolated from the NMR analyses as well. Saponite showed good sorption capacity for all selected metal ions. The regeneration of the solid sorbent after metal uptake was also analysed, obtaining encouraging results.

Introduction

Transition metal and lanthanide ions are extensively used in a wide range of scientific and technological applications, spanning from optoelectronic devices (light-emitting diodes (LEDs) or solar cells)[1,2] to diagnostic imaging (magnetic resonance (MRI) and optical imaging),[3–5] thanks to their excellent electronic, optical and magnetic properties.[6] However, their growing use worldwide brings with it some inevitable consequences.[7] Indeed, many of these metal ions can be released from medical, electronic and industrial waste and then spread into the soil or aquatic environments, thus contributing to a vast and increasing global pollution problem.[8,9] Furthermore, their accumulation in living organisms is often associated with the onset of different neurodegenerative and tumour diseases.[10–12] Recent studies have reported on a worrying release of lanthanide ions from anthropogenic sources in various urban and industrial areas worldwide, for example, in the sewage and groundwater of Berlin[13] or in San Francisco Bay.[14] The need to recover these metals and reuse them for new purposes is therefore extremely important from both environmental and economic points of view.[15,16] The recycling of these precious metal ions is of great importance and represents a scientific and technological challenge for the industrial and scientific community.

Removal of heavy metals from water/soil sources or from waste streams can be achieved by different approaches. The traditional recovery processes are based on different mechanisms, such as coagulation–flocculation, hydroxide precipitation and liquid–liquid extraction (LLE).[16,17] LLE treatments typically employ different kinds of metal chelating agents, such as ethylenediamine tetraacetic acid (EDTA), amine and amide species, to selectively capture the metals of interest.[18–23] However, these methods normally require multiple extraction steps to achieve high purity of the final product and very large amounts of expensive and dangerous extractants.[24] The development of more sustainable recovery solutions with higher efficiency, lower costs and reduced environmental impact represents an imperative challenge. A valid alternative to LLE is liquid–solid extraction (LSE),[25] based on the use of solid sorbents, such as activated carbon,[26–29] alumina or metal oxides,[30–34] porous materials,[35] metal–organic frameworks (MOFs)[36] or layered compounds.[37,38] The extraction of metal ions with these solids exploits several metal capture mechanisms (*i.e.* ion-exchange, absorption, adsorption and complexation) and has already demonstrated better selectivity, lower extraction times and potential reusability compared to conventional methods, with reduced overall operating costs.[39]

Among layered materials, natural clays have been proposed as efficient sorbents for several metal ions over the last few years, due to their low cost, chemically stable structure and

[a]*Dipartimento di Scienze e Innovazione Tecnologica, Università degli Studi del Piemonte Orientale "Amedeo Avogadro", Viale Teresa Michel 11, 15121-Alessandria, Italy. E-mail: fabio.carniato@uniupo.it, chiara.bisio@uniupo.it*
[b]*CNR-SCITEC Istituto di Scienze e Tecnologie Chimiche "G. Natta", Via C. Golgi 19, 20133-Milan, Italy*

†Electronic supplementary information (ESI) available. See DOI: 10.1039/d1dt04344g

‡These two authors contributed equally.

high cation-exchange capacity (CEC).[37,38] These lamellar systems can host high amounts of heavy metal ions (transition metals, lanthanides and actinides) in their interlayer space through ion exchange processes.[37,38,40–44] However, due to their natural origin, they usually contain several impurities in their chemical composition and possess scarcely controlled physicochemical properties. It is thus possible to avoid these disadvantages by using synthetic clays characterized by controlled morphology, particles size and physicochemical properties.[45–47] Recently, a synthetic saponite clay, belonging to the smectite family, has been studied for the recovery of lanthanide ions with different ionic radii (La^{3+}, Gd^{3+} and Lu^{3+}) from aqueous solutions, obtaining very encouraging results, especially if compared with commercial natural clays.[48] The uptake process was monitored by a conventional analytical technique, inductively coupled plasma optical emission spectroscopy (ICP-OES), which is widely used to quantify the metal concentration in different matrices.[48,49] Although this analytical technique allows for the measurement of very low concentrations of chemical elements, it requires critical pre-treatments of varying amounts of sample and destructive analyses, and therefore is not suitable for real-time metal capture evaluation.[49]

Lately, Gossuin *et al.* studied the adsorption of paramagnetic Cu^{2+} ions from aqueous solutions on alumina substrates under real-time conditions by using low-resolution ^{1}H-NMR relaxometry, as an alternative to the traditional ICP technique.[50] NMR relaxometry consists of the measurement of the longitudinal and transversal relaxation rates ($R_1 = 1/T_1$ and $R_2 = 1/T_2$, respectively) of the ^{1}H nuclei of water molecules.[51] The presence of paramagnetic ions (*i.e.* Cu^{2+}, Mn^{2+}, Co^{2+}, and lanthanide ions) in an aqueous solution can indeed decrease the R_1 and R_2 values of the water protons, through the coupling of ^{1}H magnetic moments with the paramagnetic ions. The acceleration of the relaxation rates of water protons is also proportional to the concentration of free paramagnetic ions in aqueous solution. Hence, it is therefore a suitable strategy to quantify the concentration of paramagnetic ions in solution through the analysis of R_1 and/or R_2 values.[52] Taking into account that many metal ions present in contaminated waters and waste sources show paramagnetic properties and high magnetic moments, this opens the way to the application of low-resolution NMR relaxometry in this particular scientific topic. Additionally, NMR relaxometry does not require expensive and high-field instruments and the experiments can be performed under real-time conditions with small amounts of sample and without specific pre-treatment of the matrix (further details in the Experimental section).

In this work, we evaluated the uptake capability of a Na^+-exchanged synthetic saponite clay for paramagnetic Gd^{3+}, Cu^{2+} and Co^{2+} ions in aqueous solutions (10 mM) at different pH values (5.5 and 3.0). The extraction process was followed by low-resolution ^{1}H-NMR relaxometry and confirmed by the traditional ICP-OES technique. Information on the capture process and the related kinetic parameters were extrapolated by applying dedicated mathematical models to the experimental NMR data. Moreover, the regeneration of the clay after metal ion uptake was evaluated through an exchange process in saturated NaCl solution at pH 5.5 and 2.5.

Results and discussion

Synthesis and characterization of the synthetic saponite material

Saponite (SAP) with high cationic exchange capacity and submicrometre particles was prepared by using an H_2O/Si molar ratio of 20 in the synthesis gel (Scheme S1†).[48,53] The clay was then treated with a saturated NaCl solution in order to uniformly replace all ions distributed in the interlayer space (*i.e.* Al^{3+}, Mg^{2+}, and H^+) with Na^+ ions only (Na-SAP, Scheme S1†). This procedure ensures a better chemical regularity of the exchange sites in the final sample.

The structural properties of Na-SAP were first evaluated by X-ray powder diffraction (Fig. 1A, a). The XRD pattern showed that the typical reflections of the saponite clay (Fig. 1A, a), characterised by an intense signal at 60.5° 2θ associated with the (060) plane, are typical of its 2 : 1 T–O–T structure (Fig. 1C).[45,54] The layered structure and morphology of Na-SAP were also investigated by high-resolution transmission electron microscopy (HR-TEM) (Fig. 1B). Different levels of the spatial organization of lamellae, from single crystal structures with sheet-like morphology to aggregates, are displayed in the micrograph (Fig. 1B). Moreover, the sample is composed of particles longer than 100 nm (Fig. 1B).[48,53,55]

Finally, the cationic exchange capacity (CEC) of the Na-SAP sample was evaluated *via* the UV-vis method and the value was

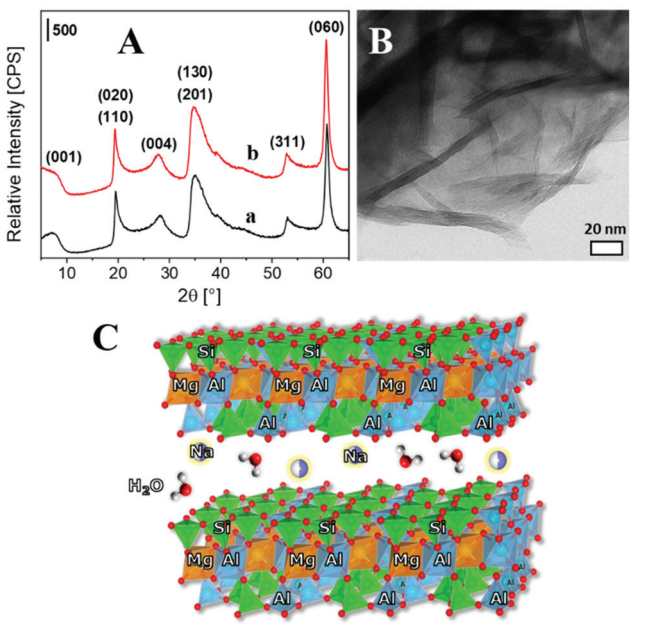

Fig. 1 (A) X-ray powder diffraction profiles of Na-SAP (a) and acid-treated Na-SAP (b). (B) HR-TEM micrographs of Na-SAP. (C) Schematic representation of the 2 : 1 T–O–T trioctahedral structure of Na-SAP.

found to be 68.2 ± 10.1 meq/100 g, which is in good agreement with the results obtained for similar synthetic saponites in the literature (Fig. S1a†).[48,53,55]

Uptake tests of Gd^{3+}, Cu^{2+} and Co^{2+} from aqueous solutions

The Na-SAP clay was tested for uptake in aqueous solutions of three different paramagnetic ions: gadolinium (Gd^{3+}), copper (Cu^{2+}) and cobalt (Co^{2+}). These chemical elements are economically-relevant, largely used in different scientific and technological fields (*i.e.* electronic devices, catalysis, and biomedicine) and their impact on the environment as potential pollutants is well known.[56] They exhibit paramagnetic properties with a magnetic moment of 7.93μ_B, 1.73μ_B and 3.88μ_B, respectively, and different ionic radii (Gd^{3+} = 1.05 Å with a coordination number (CN) of VIII, Cu^{2+} = 0.73 Å (CN = VI) and Co^{2+} = 0.65 Å (CN = VI)).[57] The metal ion capture process is based on a cation-exchange mechanism occurring between the Na^+ ions, located in the saponite interlayer space, and the paramagnetic cations in aqueous solution, which is coordinated by a variable number of inner-sphere water molecules under the pH conditions explored in this study (3.0–5.5 pH range).[58] The amount of captured elements depends on several factors: (i) the CEC of the solid, (ii) the charge and size of the metal cations and (iii) the diffusion process of the ions inside the clay galleries.[45–48,53,55]

From an experimental point-of-view, three aqueous solutions of the different metal ions (10 mM) were treated with 20 mg of Na-SAP at 298 K, directly in the NMR tube (see the Experimental section). The uptake tests were performed at acidic pH (5.5 and 3.0), under conditions that are generally adopted in commercial or industrial applications for the extraction of heavy metals from obsolete devices or metal-polluted wastewaters.[59] The NMR tubes were then inserted into a fast-field cycling (FFC) NMR relaxometer probe, operating at 0.235 T (10 MHz) and at 298 K. The metal capture process was investigated in real time without pre-treatment or further manipulation of the samples by measuring the longitudinal relaxation rate (R_1) of the aqueous solutions above the Na-SAP powder over time. By applying eqn (1) (see the Experimental section), the concentration of free metal ions in solution and, consequently, that captured by the synthetic saponite clay were calculated.[60] The relaxometric detection limit for Gd^{3+}, Cu^{2+} and Co^{2+} in water at 298 K and 10 MHz is indicated in the Experimental section.

From a visual point of view, the concentrated solutions of Cu^{2+} and Co^{2+} exhibited greenish and pink colours, respectively, while that of Gd^{3+} is colourless (Fig. S2A†). After 24 hours of treatment, the saponite powders used in the experiments with copper and cobalt displayed a colour change, from white (see photograph in Scheme S1†) to the characteristic green or pink colour of the analysed ions (Fig. S3†). Such a colour change qualitatively suggests the sequestration of the metal ions from the respective aqueous solutions.

The quantitative data of the uptake process at pH 5.5 and 3.0 are reported in Fig. 2. As a general comment, in all cases, we observed an exponential decrease of the R_1 value (shown as normalized R_1) at both pH 5.5 and 3.0, over time reaching a plateau after 5 hours, which is associated with the decrease in the concentration of free metal ions in solution. Overall, after 24 hours, the diminution of R_1 is more pronounced for the aqueous solutions treated at pH 5.5 (Fig. 2A–C). From the analysis of the R_1 values, the amounts of Gd^{3+}, Cu^{2+} and Co^{2+} ions per gram of clay (mg g^{-1}) are calculated over time and are shown in Fig. 2A′–C′. Considering both tests at different pH values, *ca.* 10–15 mg of Cu^{2+} and Co^{2+} ions per gram of saponite clay were recovered by the solid sorbent, while Gd^{3+} was captured in large amounts (25–35 mg) (Table S1†).

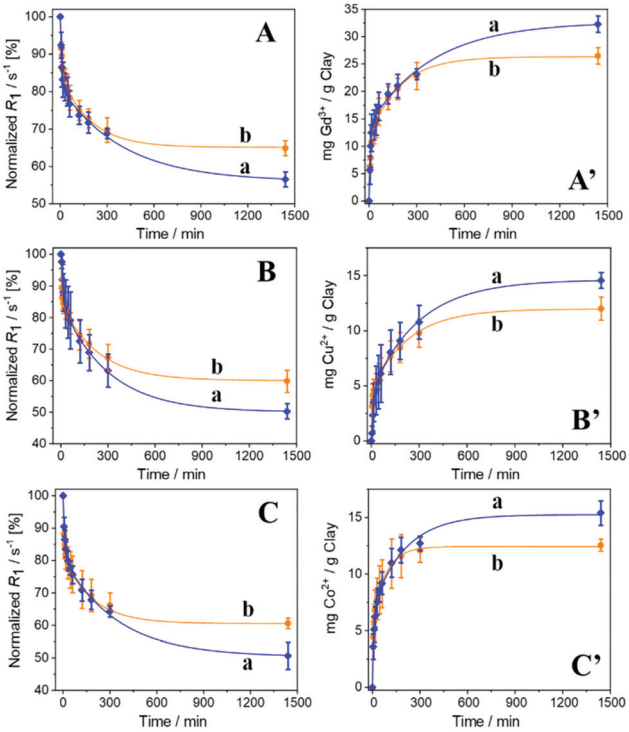

Fig. 2 Normalized R_1 values (%) (A = Gd^{3+}, B = Cu^{2+}, and C = Co^{2+}) and mg of captured metal ion per gram of Na-SAP (A′ = Gd^{3+}, B′ = Cu^{2+}, and C′ = Co^{2+}) over time. Blue curves (a, -◆-) identify the tests carried out at pH = 5.5 and orange curves (b, -●-) denote the ones at pH = 3.0.

The NMR relaxometric data were confirmed by conventional ICP-OES elemental analyses, carried out on the solutions after 24 hours of uptake (Table 1). A good correlation between the results obtained from the two techniques (expressed as mmol g^{-1}) was observed. The NMR relaxometry analyses also highlighted an increase in the concentration of metal ions extracted by the Na-SAP sample in the following order Co^{2+} > Cu^{2+} > Gd^{3+} at pH 5.5 (Table 1). By comparing the paramagnetic ions with the same charge (Cu^{2+} and Co^{2+}), Co^{2+} ions, featuring the smallest ion radius (Table S2†), were captured in greater quantities than Cu^{2+}.[57] After 24 h, Na-SAP was able to remove 0.21 mmol g^{-1} of Gd^{3+}, 0.23 mmol g^{-1} of Cu^{2+} and 0.26 mmol g^{-1} of Co^{2+} ions from the respective metal solutions at pH = 5.5 (Table 1).

There is also a noteworthy correlation between the charge of the metal ions and the amount of the exchange sites of Na-

Table 1 Uptake values after 24 h of Gd^{3+}, Cu^{2+} and Co^{2+} ions obtained from NMR relaxometry and ICP-OES elemental analyses, expressed as mmol of metal extracted per gram of Na-SAP. The saturation of exchange sites (%) with respect to the CEC of saponite is also reported

		Uptake [mmol g^{-1}]		Uptake *vs.* CEC [%]	
pH	Metal ion	NMR relaxometry	ICP-OES	NMR relaxometry	ICP-OES
5.5	Gd^{3+}	0.21 ± 0.01	0.20 ± 0.01	90 ± 4	88 ± 4
	Cu^{2+}	0.23 ± 0.01	0.24 ± 0.02	67 ± 3	70 ± 4
	Co^{2+}	0.26 ± 0.01	0.29 ± 0.02	77 ± 2	85 ± 4
3.0	Gd^{3+}	0.17 ± 0.01	0.19 ± 0.02	74 ± 4	84 ± 6
	Cu^{2+}	0.19 ± 0.02	0.19 ± 0.02	56 ± 5	53 ± 5
	Co^{2+}	0.21 ± 0.01	0.22 ± 0.03	61 ± 3	65 ± 7

SAP involved in the uptake process. For instance, Gd^{3+} ions were able to substitute more Na^+ ions in the interlayer space of Na-SAP than divalent cations, replacing almost all the available exchange sites in the clay. Indeed, as it can be noticed from Table 1, the saturation of exchange sites with respect to saponite CEC is around 90%. Conversely, for Co^{2+} and Cu^{2+} ions, these values are 77 and 67%, respectively (Table 1).

The lower overall quantity of cations captured at pH = 3.0, as shown in Table 1, is ascribed to a competition effect for exchange sites between the paramagnetic cations and the H_3O^+ ions present in the acidified metal solutions. We excluded the modifications in the structure of the saponite at pH 3.0. Indeed, the sample showed a CEC of 70.2 ± 11.9 meq per 100 g, comparable to the value calculated for Na-SAP before acid treatment. Furthermore, the X-ray pattern of acid saponite is analogous to that of Na-SAP (Fig. 1A).

The uptake kinetic was quantitatively analysed by means of a different mathematical model in order to obtain a deeper insight into the metal sequestration mechanism.[61] The best fitting of the experimental data was obtained by applying a parabolic diffusion kinetic model (Table 2),[61] thus suggesting that the capture mechanism for Na-SAP is regulated by diffusive phenomena (Fig. 3 and S4†). The model is defined by eqn (2), described in detail in the Experimental section.

By fitting the NMR data with the mathematical model, it was possible to extrapolate the rate constants (k) for all the uptake experiments (Table 2). The metal ion sequestration process appeared faster for Co^{2+} ions (k = 0.4588 s^{-1} at pH = 5.5), which has the smallest ionic radius between the three metals studied (Table 2). In addition, at pH = 3.0, the process is accelerated for both Co^{2+} and Cu^{2+} uptakes.

Table 2 Kinetic constant rate (k) and coefficient of determination (R^2) obtained after linear fitting of NMR relaxometric data, referred to Gd^{3+}, Cu^{2+} and Co^{2+} sorption shown in Fig. 3 and S4,† with the parabolic diffusion kinetic model[61]

pH	Gd^{3+}	Cu^{2+}	Co^{2+}
5.5	k = 0.3136 s^{-1}	k = 0.3541 s^{-1}	k = 0.4588 s^{-1}
	R^2 = 0.9599	R^2 = 0.9646	R^2 = 0.9961
3.0	k = 0.3089 s^{-1}	k = 0.4044 s^{-1}	k = 0.5590 s^{-1}
	R^2 = 0.9932	R^2 = 0.9877	R^2 = 0.9914

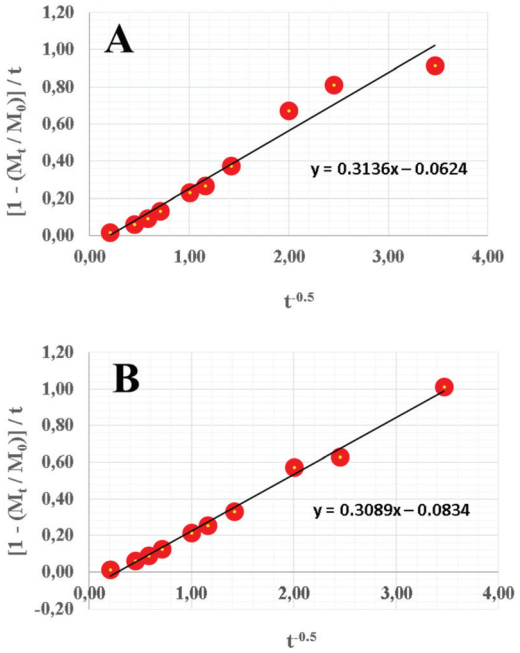

Fig. 3 Fitting of the NMR relaxometric data with the parabolic diffusion kinetic model[61] for the sorption of Gd^{3+} ions at pH = 5.5 (A) and 3.0 (B).

Regeneration of Na-SAP clay and recovery of heavy metal ions

The evaluation of the regeneration capacity of the solid sorbent after the removal of metal ions from aqueous solutions is undoubtedly another important parameter to be analysed. Elimination of the exchanged metal ions was performed by treating the paramagnetic clays obtained after the uptake tests with a saturated NaCl solution, through a retro-exchange mechanism,[48] at a weakly acidic pH (pH = 5.5) and under more acid conditions (pH = 2.5). The regeneration test was applied to the Na-SAP solids after 24 h of metal ion uptake at pH = 5.5. The treatment was replicated three times on the same solid. The solutions derived from these regeneration cycles were measured with NMR relaxometry at 10 MHz and 298 K.

After three recovery cycles, the coloured solids containing Cu^{2+} and Co^{2+} showed a marked reduction of their colour at both pH values (Fig. S3†), thus visually indicating the release of metal ions from Na-SAP.

The amounts of Gd^{3+} ions recovered from Na-SAP after each cycle in NaCl solutions at pH = 5.5 and 2.5 are reported in Fig. 4. After the first recovery cycle, more than 40% of the Gd^{3+} ions were recovered from the clay with respect to the total amount intercalated in the solid (Fig. 4). Subsequent recovery cycles led only to a slight increase in the number of ions released in the solution (Fig. 4). Similar results were obtained for the regeneration test carried out at pH = 2.5.

The same procedure was applied to saponite clays containing Co^{2+} and Cu^{2+} ions after 24 h of uptake. The overall quantity of ions recovered at the end of all cycles was much larger

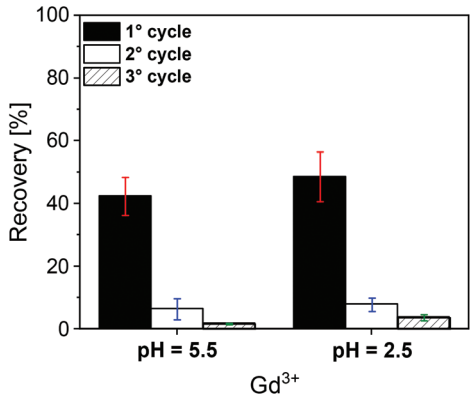

Fig. 4 Gd^{3+} ion release (%) from Na-SAP after uptake for 24 h at pH 5.5. The regeneration test was repeated for 3 cycles in saturated NaCl solutions at pH = 5.5 and 2.5.

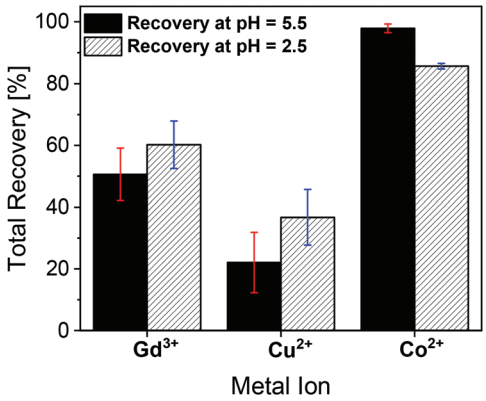

Fig. 5 Gd^{3+}, Cu^{2+} and Co^{2+} release (%) after 3 regeneration tests of Na-SAP after uptake for 24 h at pH 5.5. The release of the metal ions was carried out at pH 5.5 (black bars) and 2.5 (white bars).

for Co^{2+} (*ca.* 90%) than for Cu^{2+} (*ca.* 20%) (Fig. 5, Table S3†). This different behaviour is attributed to the different ionic radii of the two cations, which is smaller for Co^{2+} than for Cu^{2+} ion. However, other reasons related to diffusion phenomena occurring during the regeneration process, which are difficult to monitor and analyse, are not to be excluded. Similar behaviour and results were observed for the samples regenerated at pH 2.5.

Conclusions

The uptake of paramagnetic heavy metal ions with different charges and ionic radii (Gd^{3+}, Cu^{2+} and Co^{2+}) from aqueous solutions has been evaluated by exploiting a Na^{+}-exchanged synthetic saponite clay with micrometre-sized particles and high cation-exchange capacity as a sorbent. The heavy metal ion removal was monitored in real time, without pre-treatment of the sample, by ^{1}H-NMR relaxometry and the method was confirmed by conventional ICP-OES techniques. The excellent agreement of the data across the two approaches proved that ^{1}H NMR relaxometry is a versatile methodology suitable for this study, with the following important advantages: (i) it does not require expensive equipment, (ii) it can be applied to monitor the uptake process under real-time conditions and (iii) it can be applied to study low amounts of samples (a few milligrams), without manipulation or pre-treatment of the matrix.

The uptake results demonstrated that the Na-SAP clay is a promising cation exchanger, which is able to remove from water appreciable amounts of di- and trivalent ions. The best uptake results were obtained for Co^{2+} ions (0.26 mmol g^{-1} corresponding to 15.4 mg g^{-1}) at pH 5.5 after 24 h of contact with the paramagnetic solution.

Finally, the regeneration tests in saturated NaCl solutions at pH 5.5 and 2.5 were applied to Na-SAP in order to remove the previously captured metal ions. The results were encouraging, with the recovery of metal ions spanning from *ca.* 20% for Cu^{2+} to *ca.* 90% for Co^{2+}. In conclusion, synthetic saponite clays have proven to be very good materials for removing heavy metal ions from aqueous environments.

Experimental section

Materials

Synthesis of Na-SAP clay. The Na^{+}-exchanged synthetic saponite clay was prepared using a hydrothermal method, optimized in our laboratories.[48,53,55] 5.95 g of fumed SiO_2 was introduced in 29.1 mL of 0.4 M NaOH solution. The gel was stirred at 298 K for 1 h. 18.8 g of magnesium acetate tetrahydrate, 2.3 g of aluminium isopropoxide and 8.2 mL of ultrapure water were added to the gel. After stirring for 2 h, the mixture was introduced in an autoclave and treated at 513 K for 72 h. The final solid (SAP) was filtered and washed with ultrapure water. 2 g of the SAP sample was dispersed in 200 mL of saturated NaCl solution for 36 h at 298 K. This procedure allows the replacement of the cations present in the interlayer space (*i.e.*, Al^{3+}, Mg^{2+}, and H^{+}) with Na^{+}. The final sample (Na-SAP) was finally filtered, washed with hot ultrapure water and dried at 100 °C overnight.

Gd^{3+} solution (10 mM). 186.1 mg of $GdCl_3{\cdot}6H_2O$ was dissolved in 50 mL of ultrapure water, obtaining a colourless solution. The pH was corrected to 5.5 with a few drops of 1 M NaOH. 25 mL of this solution was also acidified to pH = 3.0 with HNO_3 solution (0.01 M).

Cu^{2+} solution (10 mM). 85.0 mg of $CuCl_2{\cdot}2H_2O$ was dissolved in 50 mL of ultrapure water, obtaining a slightly blue solution. The pH correction to 5.5 and 3.0 was realized by following the same approach that was adopted for Gd^{3+} solution preparation.

Co^{2+} solution (10 mM). 64.3 mg of anhydrous $CoCl_2$ was dissolved in 50 mL of ultrapure water, obtaining a slightly pink solution. The pH was corrected to 5.5 and 3.0 with diluted NaOH and HNO_3 solutions (see above).

Saturated NaCl solutions. 36 g of NaCl was dissolved in 100 mL of ultrapure water and stirred for 24 h at 298 K; the pH of the solution was then corrected to 5.5 with 0.01 M HNO_3 and to 2.5 with 0.1 M HNO_3.

Uptake test in aqueous solutions

20 mg of Na-SAP was introduced in 10 mm NMR tubes and 1 mL of 10 mM aqueous solutions of Gd^{3+}, Cu^{2+} or Co^{2+} at pH = 5.5 and 3.0 was carefully added to each tube in order to avoid suspension of the powder. Each sample so-prepared was inserted into the probe of a Fast-Field Cycling (FFC) Stelar SmarTracer Relaxometer. The R_1 values of the aqueous solution above the solid fraction were measured at 10 MHz and 298 K under static conditions over time.

The concentration of the free metal ions in solution during the uptake process was calculated by eqn (1) (ref. 60), where R_1 (s^{-1}) is the ^1H longitudinal relaxation rate of the paramagnetic solution, R_{1d} corresponds to the diamagnetic contribution of pure water (0.38 s^{-1} at 298 K and 10 MHz) and r_1 (mM^{-1} s^{-1}) is the relaxivity parameter typical of each metal aquo-ion. The r_1 values are 17.9, 1.3 and 0.14 mM^{-1} s^{-1} for $[Gd(H_2O)_8]^{3+}$, $[Cu(H_2O)_6]^{2+}$ and $[Co(H_2O)_6]^{2+}$ at 298 K and 10 MHz, respectively.[62] The relaxometric detection limits for Gd^{3+}, Cu^{2+} and Co^{2+} in water at 298 K and 10 MHz are approximately 0.01, 0.1 and 0.9 mM, respectively.

$$r_1 = \frac{R_1 - R_{1d}}{[\text{metal}]} \quad (1)$$

The uptake values after 24 h for each metal ion at each pH value were then compared with those obtained by measuring the same solutions, after centrifugation and separation, by ICP-OES elemental analysis.

Analysis of uptake kinetics

The experimental NMR data collected over time were analysed by different kinetic models: (1) the zero-order model, (2) the first-order model, (3) Bhaskar's equation, (4) parabolic diffusion and (5) a modified Freundlich model. The description of each mathematical approach is reported in detail in the literature.[61] The uptake data analysis results were consistent with the parabolic diffusion mathematical model, which described the diffusion-controlled event in clays. This model is defined by the following eqn (2):[61]

$$1 - \frac{\frac{M_t}{M_0}}{t} = -k_p t^{-0.5} + m \quad (2)$$

where M_0 and M_t are the concentrations (in mM) of paramagnetic metal ions (Gd^{3+}, Cu^{2+} or Co^{2+}) that remained in aqueous solution at time 0 (at the start of the test) and at different times t (from 5 min to 24 h), respectively, k is the rate constant of the uptake process and m is a constant.[61]

By the application of this model, it was possible to extrapolate the kinetic constants of the ion-exchange processes for all tests performed in this study.

Regeneration of the solids in saturated NaCl solutions

The Na-SAP solids after metal ion uptake at pH = 5.5 for 24 h were first dried in an oven at 343 K overnight and then dispersed in 1 mL of a saturated NaCl solution, at two different pH values of 5.5 and 2.5. The suspensions were sonicated for 1 h at 59 kHz and 313 K and then centrifuged to separate the powder from the solution. The treatment in NaCl solution was consecutively repeated for three regeneration cycles on the same solid. The liquid fractions after each regeneration step were analysed by ^1H-NMR relaxometry at 10 MHz and 298 K. The concentrations of the metal ions released in solution were then calculated by applying eqn (1).

Characterisation methods

Elemental analyses were performed using an Ametek Spectro Genesis EOP ICP-OES equipped with a cross-flow nebulizer, with simultaneous spectrum capture in the 175–770 nm wavelength range. The aqueous solutions were opportunely diluted in 1 wt% HNO_3 before analysis.

X-ray powder diffractograms (XRPD) were collected on unoriented ground powders using a Bruker D8 Advance powder diffractometer equipped with a Linxeye XE-T detector. The X-ray tube operates with Cu-$K_{\alpha1}$ (λ = 1.54062 Å) monochromatic radiation and the operative electric potential difference and current intensity are set to 40 kV and 40 mA, respectively. The variable primary divergent slits and the primary and secondary Soller slits are 2.5°. The diffractograms were recorded at RT in the 5°–65° 2θ range and with the following settings: coupled-$2\theta - \theta$ method, fast and continuous scan mode, time per step (rate) of 0.05° min^{-1}, increment (step size) of 0.02° and automatic air scatter and slits.

High-resolution transmission electron microscope (HR-TEM) micrographs of the Na-SAP-20 sample were collected using a Zeiss libra200 FE3010 high resolution transmission electron microscope operating at 200 kV. The specimen was prepared by depositing the sample on carbon-coated grids.

The cationic exchange capacity (CEC) of the synthetic saponite was determined by the UV-vis method as reported in the literature.[63] In details, 0.300 g of Na-SAP was exchanged with 10 mL of a 0.02 M hexaamminecobalt(III) chloride ($[Co(NH_3)_6]^{3+}$) solution at 298 K for 60 h. After separation by centrifugation, the solution was analysed by UV-vis spectroscopy. The UV-vis spectra were recorded at 298 K in the range 300–600 nm with a resolution of 1 nm using a double-beam PerkinElmer Lambda 900 spectrophotometer. The absorbance of the band at 475 nm ($^1A_{1g} \rightarrow {}^1T_{1g}$),[64] relative to a d–d spin-allowed Laporte-forbidden transition of Co^{3+}, was evaluated to quantify the amount of free Co^{3+} ions in solution, thereby determining the amount exchanged in the procedure and thus the CEC of the saponite sample. $[Co(NH_3)_6]^{3+}$ standard aqueous solutions, in the concentration range of 0.05–0.005 M, were measured at room temperature.

The water proton longitudinal relaxation rates (R_1) were measured by using a Fast-Field Cycling (FFC) Stelar SmarTracer Relaxometer operating over a range of magnetic field strengths from 0.00024 to 0.25 T (0.01–10 MHz proton Larmor frequencies range). The measurements were carried out using a standard non-polarized NP/S sequence with a typical 90° pulse width of 3.5 μs and reproducibility of data within ±0.5%. The temperature was controlled using a Stelar

VTC-91 heater airflow equipped with a copper-constantan thermocouple (uncertainty of ±0.1 °C).

Author contributions

Conceptualization, S. M., S. N., C. B. and F. C.; methodology, S. M., S. N., C. B. and F. C.; formal analysis, S. M., S. N. and M. G.; investigation, S. M. and S. N.; data curation, S. M. and S. N.; writing—original draft preparation, S. M. and S. N.; writing—review and editing, M. G., C. B. and F. C. All authors have read and agreed to the published version of the manuscript.

Conflicts of interest

There are no conflicts to declare.

Acknowledgements

The authors gratefully thank Dr Claudio Evangelisti (CNR-SCITEC, Milan, Italy) for the collection of HR-TEM micrographs, Dott. Chiara Zaccone and Dr Elena Perin (DiSIT, Università del Piemonte Orientale, Alessandria, Italy) and Dr Marcello Marelli (CNR-SCITEC, Milan, Italy) for ICP-OES analyses. Financial support from the Università del Piemonte Orientale (FAR – 2019) is also acknowledged.

Notes and references

1 S. Massari and M. Ruberti, *Resour. Policy*, 2013, **38**(1), 36–43.
2 J.-C. G. Bünzli, *Coord. Chem. Rev.*, 2015, **293–294**, 19–47.
3 A. F. Mingo, S. C. Serra, S. Baroni, C. Cabella, R. Napolitano, I. Hawala, I. M. Carnovale, L. Lattuada, F. Tedoldi and S. Aime, *Magn. Reson. Med.*, 2016, **78**(4), 1523–1532.
4 (*a*) D. Parker, *Handbook on the Physics and Chemistry of Rare Earths*, ed. J.-C. G. Bünzli and V. K. Pecharsky, Elsevier, Amsterdam, 2016, 50, pp. 269–299, ISBN: 978-0-444-63851-9; (*b*) O. L. Andersen, J. Madsen, U. K. Poulsen, O. Jepsen and J. Kollár, *Physica B+C*, 1977, **86–88**(Part 1), 249–256.
5 F. Carniato, L. Tei and M. Botta, *Eur. J. Inorg. Chem.*, 2018, **46**, 4936–4954.
6 (*a*) V. Balzani, P. Ceroni and A. Juris, *Photochemistry and Photophysics: Concepts, Research, Applications*, Wiley-VCH Verlag GmbH & Co, Weinheim, 2014, ISBN: 978-3-527-33479-7; (*b*) E. P. Beaumier, A. J. Pearce, X. Y. See and I. A. Tonks, *Nat. Rev. Chem.*, 2019, **3**, 15–34.
7 (*a*) R. Ronda, T. Jüstel and H. Nikol, *J. Alloys Compd.*, 1998, **275–277**, 669–676; (*b*) J. Malinowski, D. Zych, D. Jacewicz, B. Gawdzik and J. Drzeżdżon, *Int. J. Mol. Sci.*, 2020, **21**, 5443–5468.
8 H. Herrmann, J. Nolde, S. Berge and S. Heise, *Ecotoxicol. Environ. Saf.*, 2016, **124**, 213–238.
9 G. Klaver, M. Verheul, I. Bakker, E. Petelet-Giraud and P. Négrel, *Appl. Geochem.*, 2014, **47**, 186–197.
10 L. Leyssens, B. Vinck, C. Van Der Straeten, F. Wuyts and L. Maes, *Toxicology*, 2017, **387**, 43–56.
11 P. B. Tchounwou, C. G. Yedjou, A. K. Patlolla and D. J. Sutton, *Molecular, Clinical and Environmental Toxicology, Experientia Supplementum*, ed. A. Luch, Springer, Basel, 2021, 101, pp. 133–164, ISBN: 978-3-7643-8340-4.
12 R. K. Sharma and M. Agrawal, *J. Environ. Biol.*, 2005, **26**, 301–313.
13 A. Knappe, P. Möller, P. Dulski and A. Pekdeger, *Chem. Erde-Geochem.*, 2005, **65**(2), 167–189.
14 V. Hatje, K. W. Bruland and A. R. Flegal, *Environ. Sci. Technol.*, 2016, **50**(8), 4159–4168.
15 (*a*) O. B. Akpor, *Adv. Biosci. Bioeng.*, 2014, **2**, 37; (*b*) M. Athar and S. B. Vohora, *Man and environment series*, ed: P. K. Ray, Wiley Eastem Ltd., New Delthi, 1995, pp. 1–195; (*c*) S. Sharma, *Heavy Metals In Water: Presence, Removal and Safety*, RSC Publishing, 2015, ISBN: 978-1-84973-885-9.
16 (*a*) A. Tsamis and M. Coyne, Recovery of Rare Earths from Electronic Wastes: An Opportunity for High-Tech SMEs, *European Parliament, Directorate-General for Internal Policies of the Union*, 2015; (*b*) F. Fu and Q. Wang, *J. Environ. Manage*, 2011, **92**, 407–418; (*c*) M. Muchie and O. B. Akpor, *Int. J. Phys. Sci.*, 2010, **5**, 1807–1817.
17 N. Swain and S. Mishra, *J. Cleaner Prod.*, 2019, **20**, 884–898.
18 A. Roca-Sabio, M. Mato-Iglesias, D. Esteban-Gòmez, E. Tòth, A. de Blas, C. Platas Iglesias and T. Rodríguez-Blas, *J. Am. Chem. Soc.*, 2009, **131**, 3331–3341.
19 L. Tei, Z. Baranyai, E. Breucher, C. Cassino, F. Demicheli, N. Masciocchi, G. B. Giovenzana and M. Botta, *Inorg. Chem.*, 2010, **49**, 616–625.
20 J. Florek, A. Mushtaq, D. Larivière, G. Cantin, F.-G. Fontaine and F. Kleitz, *RSC Adv.*, 2015, **5**(126), 103782–103789.
21 A. Leoncini, P. K. Mohapatra, A. Bhattacharyya, D. R. Raut, A. Sengupta, P. K. Verma, N. Tiwari, D. Bhattacharyya, S. Jha, A. M. Wouda, J. Huskens and W. Verboom, *Dalton Trans.*, 2016, **45**(6), 2476–2484.
22 P. Kishor, A. Sengupta, N. K. Gupta and S. Biswas, *Sep. Sci. Technol.*, 2017, **53**(2), 286–294.
23 Y. Hu, E. Drouin, D. Larivière, F. Kleitz and F.-G. Fontaine, *ACS Appl. Mater. Interfaces*, 2017, **9**(44), 38584–38593.
24 P. Anastas and N. Eghbali, *Chem. Soc. Rev.*, 2010, **39**(1), 301–312.
25 E. P. Horwitz, R. Chiarizia, M. L. Dietz, H. Diamond and D. M. Nelson, *Anal. Chim. Acta*, 1993, **281**(2), 361–372.
26 A. bin Jusoh, W. H. Cheng, W. M. Low, A. Nora'aini and M. J. Megat Mohd Noor, *Desalination*, 2005, **182**, 347–353.
27 M. Kobya, E. Demirbas, E. Senturk and M. Ince, *Bioresour. Technol.*, 2005, **96**, 1518–1521.

28 P. Mondal, C. Balomajumder and B. Mohanty, *J. Hazard. Mater.*, 2007, **144**, 420–426.
29 L. Monser and N. Adhoum, *Sep. Purif. Technol.*, 2002, **26**, 137–146.
30 M. Hua, S. Zhang, B. Pan, W. Zhang, L. Lv and Q. Zhang, *J. Hazard. Mater.*, 2021, **211–212**, 317–331.
31 K. G. Karthikeyan, H. A. Elliott and F. S. Cannon, *Environ. Sci. Technol.*, 1997, **31**, 2721–2725.
32 M. B. McBride, *Clays Clay Miner.*, 1982, **30**, 21–28.
33 M. Okazaki, K. Takamidoh and I. Yamane, *Soil Sci. Plant Nutr.*, 1986, **32**, 523–533.
34 E. P. Legaria, S. D. Topel, V. G. Kessler and G. A. Seisenbaeva, *Dalton Trans.*, 2015, **44**(3), 1273–1282.
35 P. D. Hopkins, T. Mastren, J. Florek, R. Copping, M. Brugh, K. D. John, M. F. Nortier, E. R. Birnbaum, F. Kleitz and M. E. Fassbender, *Dalton Trans.*, 2018, **47**(15), 5189–5195.
36 X. Zhao, M. Wong, C. Mao, T. X. Trieu, J. Zhang, P. Feng and X. Bu, *J. Am. Chem. Soc.*, 2014, **136**, 12572–12575.
37 (*a*) A. Alshameri, H. He, C. Xin, J. Zhu, W. Xinghu, R. Zhu and H. Wang, *Hydrometallurgy*, 2019, **185**, 149–161; (*b*) L. Petra, P. Billik, Z. Melichová and P. Komadel, *Appl. Clay Sci.*, 2017, **143**, 22–28.
38 (*a*) D. R. Fröhlich, *Clays Clay Miner.*, 2015, **63**, 262–276; (*b*) M. Cruz-Guzmán, R. Celis, M. C. Hermosín, W. C. Koskinen, J. Nater and E. A. Cornejo, *Soil Sci. Soc. Am. J.*, 2006, **70**, 215–221.
39 E. Juère, J. Florek, D. Larivière, J. Kim and F. Kleitz, *New J. Chem.*, 2016, **40**(5), 4325–4334.
40 (*a*) P. O. Pastor, E. R. Castellon and A. Rodriguez, *Solvent Extr. Ion Exch.*, 1987, **5**, 1151–1169; (*b*) C. Chen, H. Liu, T. Chen, D. Chena and R. L. Frost, *Appl. Clay Sci.*, 2015, **118**, 239–247.
41 P. Olivera-Pastor, E. Rodriguez-Castellon and A. Rodríguez García, *Clays Clay Miner.*, 1988, **36**(1), 68–72.
42 E. Tertre, G. Berger, E. Simoni, S. Castet, E. Giffaut, M. Loubet and H. Catalette, *Geochim. Cosmochim. Acta*, 2006, **70**(18), 4563–4578.
43 N. Finck, M. L. Schlegel and D. Bosbach, *Environ. Sci. Technol.*, 2009, **43**(23), 8807–8812.
44 E. Galunin, M. D. Alba, M. J. Santos, T. Abrao and M. Vidal, *J. Hazard. Mater.*, 2011, **186**(2–3), 1930–1941.
45 (*a*) C. H. Zhou, Q. Zhou, Q. Q. Wu, S. Petit, X. C. Jiang, S. T. Xia, C. S. Li and W. H. Yu, *Appl. Clay Sci.*, 2019, **168**, 136–154; (*b*) F. Carniato, G. Gatti and C. Bisio, *New J. Chem.*, 2020, **44**, 9969–9980.
46 (*a*) S. Marchesi, F. Carniato, C. Bisio, L. Tei, L. Marchese and M. Botta, *Dalton Trans.*, 2018, **47**(24), 7896–7904; (*b*) D. Lalli, S. Marchesi, F. Carniato, C. Bisio, L. Tei, L. Marchese and M. Botta, *Dalton Trans.*, 2020, **49**, 6566–6657.
47 (*a*) S. Marchesi, C. Bisio and F. Carniato, *RSC Adv.*, 2020, **10**, 29765–29771; (*b*) S. Marchesi, M. Guidotti, L. Marchese, C. Evangelisti, F. Carniato and C. Bisio, *Chem. – Eur. J.*, 2021, **27**, 4723–4730; (*c*) S. Marchesi, C. Bisio, D. Lalli, L. Marchese, C. Platas-Iglesias and F. Carniato, *Inorg. Chem.*, 2021, **60**(14), 10749–10756; (*d*) S. Marchesi, C. Bisio and F. Carniato, *Appl. Sci.*, 2021, **11**(19), 8903–8914.
48 S. Marchesi, F. Carniato, M. Guidotti, M. Botta, L. Marchese and C. Bisio, *New J. Chem.*, 2020, **44**, 10033–10041.
49 K. Jayanta, K. Smita, D. Sarla and R. Rajeev, *J. Metall. Mater. Sci.*, 2018, **60**(1), 21–24.
50 Y. Gossuin and L. Vuong, *Sep. Purif. Technol.*, 2018, **202**, 138–143.
51 (*a*) I. Foley, S. A. Farooqui and R. L. Kleinberg, *J. Magn. Reson., Ser. A*, 1996, **123**(1), 95–104; (*b*) S. H. Koenig and R. D. Brown III, *Magn. Reson. Med.*, 1984, **1**(4), 478–495.
52 (*a*) R. Kimmich, *Field-cycling NMR Relaxometry: Instrumentation, Model Theories and Applications*, 2019, RSC Publishing, ISBN: 978-1-78801-154-9; (*b*) R. M. Steele, J.-P. Korb, G. Ferrante and S. Bubici, *Magn. Reson. Chem.*, 2015, **54**(6), 502–509; (*c*) S. M. Nagel, C. Strangfeld and S. Kruschwitza, *J. Magn. Reson. Open*, 2021, **6–7**, 100012.
53 D. Costenaro, G. Gatti, F. Carniato, G. Paul, C. Bisio and L. Marchese, *Microporous Mesoporous Mater.*, 2012, **162**, 159–167.
54 J. Roosen, J. Spoorenand and K. Binneman, *J. Mater. Chem. A*, 2014, **2**(45), 19415–19426.
55 C. Bisio, G. Gatti, E. Boccaleri, G. B. Superti, H. O. Pastore and M. Thommes, *Microporous Mesoporous Mater.*, 2008, **107**, 90–101.
56 (*a*) G. Pagano, M. Guida, F. Tommasi and R. Oral, *Ecotoxicol. Environ. Saf.*, 2015, **115**, 40–48; (*b*) J. P. Vareda, A. J. M. Valente and L. Duraes, *J. Environ. Manage.*, 2019, **246**, 101–118.
57 (*a*) R. D. Shannon, *Acta Crystallogr., Sect. A: Cryst. Phys., Diffr., Theor. Gen. Crystallogr.*, 1976, **32**, 751; (*b*) D. F. Shriver and P. Atkins, *Inorganic Chemistry*, Oxford University Press, New York, 5th edn, 2010.
58 (*a*) K. J. Powell, P. L. Brown, R. H. Byrne, T. Gajada, G. Hefter, S. Sjoberg and H. Wanner, *Pure Appl. Chem.*, 2007, **79**, 895–950; (*b*) H. M. H. Gad, H. A. Omar, M. Aziz, M. R. Hassan and M. H. Khalil, *Asian J. Chem.*, 2016, **28**, 385–394; (*c*) P. Djurdjevi, R. Jeli, L. Joksovi, I. Lazarevi and M. Jeliki-Stankov, *Acta Chim. Slov.*, 2010, **57**, 386–397.
59 R. W. Gaikwad and D. V. Gupta, *Appl. Ecol. Environ. Res.*, 2008, **6**, 81–98.
60 S. Aime, M. Botta, M. Fasano and E. Terreno, *Chem. Soc. Rev.*, 1998, **27**, 19–29.
61 H. Zhang, D. Pan and X. Duan, *J. Phys. Chem. C*, 2009, **113**, 12140–12148.
62 (*a*) C. Luchinat, *Magn. Reson. Chem.*, 1993, **31**, S145–Sl53; (*b*) K. Micskei, D. H. Powell, L. Helm, E. Brücher and A. Merbach, *Magn. Reson. Chem.*, 1993, **31**, 1011–1020.
63 O. Prieto, M. A. Vincente and M. A. Banares-Munoz, *J. Porous Mater.*, 1999, **6**, 335–344.
64 J. C. Dabrowiak, *Metals in Medicine*, John Wiley & Sons Ltd, 2nd edn, 2017, ISBN: 978-1-119-19130-8.